

# Chaotic behavior of micro quasar GRS 1915+105

Banibrata Mukhopadhyay

*Astronomy Division, University of Oulu, P.O.Box 3000, FIN-90014, Finland*

## Abstract.

Black hole binaries are variable in timescales of range from months to milli-seconds. The origin of this variability is still not clear, it could be due to the variation of external parameters, like mass accretion rate, instabilities in the inner regions of the accretion flow etc. Important constraints on these possibilities can be obtained from the study of the non-linear behavior of fluctuations. We present a modified non-linear time series analysis technique which optimizes the use of the available data and computes the correlation dimension in a non-subjective manner. We apply this technique to the X-ray light-curve of the black hole system, GRS 1915+105, to show conclusively that at least for four of its twelve temporal classes, the underlying mechanism is a low order chaotic one.

## 1. INTRODUCTION

One of the most interesting black hole candidates observed so far is GRS 1915+105. Like other black hole sources, it shows the X-ray variability in a wide range of timescale varies from months to milli-seconds, which certainly indicates that the system is highly non-linear (that is even true for other black holes). However, the most exciting thing behind this micro quasar GRS 1915+105 is that, according to the temporal variability it can be classified into twelve different temporal classes with respect to the morphology of light-curves for different observation IDs (OIDs) [1]. But, from this temporal classification one is unable to understand about a basic feature of non-linearity, whether this black hole is a random or chaotic system, that is our present goal to understand. Following an established technique of non-linear dynamical physics applied earlier to other related astrophysical problems [2, 3, 4], here we plan to establish that the micro quasar GRS 1915+105 as well as the black system is chaotic in nature. This analysis of temporal behavior of a system plays an important role to understand the geometry of the source, which thus eventually be used to test its relativistic nature and the corresponding accretion process.

Before going into detail of our analysis, let us introduce some basic definitions of various terminology used in this article.

**Chaos:** If any two consecutive trajectories of a system, while divergent each other, are related by some law, the system is called chaotic (eventhough instantaneously it looks like random but overall it is deterministic). Brownian motion is an immediate prac-

tical example of it. In case of the accretion disk physics, one can check this by investigating various orbits around a compact object.

**Random:** If any two consecutive trajectories of a system are not related by any physics, the system is called random. Poisson noise is an example.

**Degrees of Freedom:** From the concept of classical mechanics, the *Free Degrees of Freedom* of an  $M$  dimensional system is  $M$ . If the number of constraints into the system is  $n$ , the *Net Degrees of Freedom* of the same system can be defined as,  $D = M - n$ . Philosophically, same thing is true even in the case of non-linear dynamics, however, the estimated  $D$  need not be integer (unlike any classical mechanical system). In non-linear dynamics,  $D$  is the measure of chaos, called *chaotic dimension* of the system. If there is no constraint into the system at any dimension,  $M$ ;  $D = M$ , both the degrees of freedom are same, and therefore the system is random. Naturally, for a constraintless random system  $D$  varies linearly with  $M$  while for a chaotic system  $D$  saturates to a value above the particular  $M$ . For an ideal chaotic system,  $D$  saturates when  $M \geq 2$ , thus sometimes denoted as  $D_2$ .

The chaotic nature of accretion phenomena in magneto-hydrodynamic simulations has been found by Winters et al. [5] already. Therefore we are motivated to check this chaotic nature from the observational point of view, analyzing black holes data. If the fluctuations in an accretion disk is random or stochastic, the corresponding X-ray variations are expected due to the variation of external parameters, e.g. accretion rate, and/or there is a possibility of random flares and vice versa. In contrary,

the presence of chaotic nature, which is deterministic, may be due to the inner disk instability and/or coherent flares and vice versa.

To determine the chaotic nature of GRS 1915+105, in the next section, we outline the methodology and in §3 discuss results for different OIDs. Finally in §4, we make our conclusions.

## 2. METHOD

Once we have the light-curve data, let us denote the count rate at the time  $t_j$  be  $s(t_j)$ . Let us also identify a *delay*,  $\tau$ , that indicates the time interval beyond which any two count rates are not related. This is the time at which the auto-correlation function of the system goes to zero or reaches to its first minima (if it does not go to zero). If the auto-correlation function neither goes to zero nor attains a minimum, the mentioned *delay time* has to be figured out in a different way explained in §3. Therefore, using this delay one can construct a vector at time  $t_j$  in an  $M$  dimensional space as

$$\vec{x}_j = \vec{x}(t_j) = \{s(t_j), s(t_j + \tau), s(t_j + 2\tau), \dots \text{up to } M^{\text{th}} \text{ s}\}. \quad (1)$$

In this way all the possible  $M$  dimensional vectors have to be constructed for  $j = 1, 2, 3, \dots, N$ , and one can get an  $N \times M$  matrix equation. Then one has to map all the vectors in an  $M$  dimensional phase-portrait, and to compute the average number of data points within a distance  $R$  from a particular data point<sup>1</sup>. For example, in case of  $M = 2$ , one has to find out that mentioned average number of points in the  $s(j + \tau) - s(j)$  space. This is called the correlation sum, defined as

$$C_M(R) = \lim_{N \rightarrow \infty} \frac{1}{N(N-1)} \sum_i^N \sum_{j \neq i}^N H(R - |\vec{x}_i - \vec{x}_j|), \quad (2)$$

where  $H(R - |\vec{x}_i - \vec{x}_j|)$  is a Heaviside step function. Then one has to find out  $C_M(R)$  for different  $R$ s. Finally, the whole process has to repeat for the various choices of  $M$  (say  $1 \rightarrow 15$ ). Subsequently, the variation of  $\log[C_M(R)]$  as a function of  $\log[R]$  when  $M$  is a parameter, has to be seen concentrating on the (approximate) linear region of curves. Finally the average slope of approximate linear region of the curve for different  $M$  to be computed as the correlation dimension of the system, defined as

$$D_2 = \frac{d[\log C_M(R)]}{d[\log(R)]}. \quad (3)$$

Now from the variation of  $D_2$  as a function of  $M$ , one can understand whether the system is chaotic or random

<sup>1</sup> The average number of data points in an  $M$ -cube of arm length  $R$  or  $M$ -sphere of radius  $R$  in the phase-portrait.

as mentioned in §1, and the chaotic dimension can be identified from the saturated value of  $D_2$  in the curve. The details of all these will be presented elsewhere [6].

An important point to be noted here that for a very small  $R$  ( $\leq R_{min}$ ),  $C_M(R)$  would be of the order of unity and the result would be Poisson noise dominated. On the other hand, for a large  $R$  ( $\geq R_{max}$ ),  $C_M(R)$  would saturate to the total number of data points. Therefore for a particular  $M$ , there is a range of  $R$  which gives the physical result where the  $C_M(R) - R$  curve is linear. Also the maximum  $M$  (largest  $M$ -cube/sphere) is chosen in such a manner that it has to be within the embedding space so that filled by points and there should not be any edge effect due to the limitation of point's number. Due to all these mentioned reasons, if  $M$  is above of a particular value  $M_c$  ( $M > M_c$ ) there is a chance that  $R_{min} = R_{max}$ , and then no significant results can be obtained.

Now we like to apply all the above mentioned technique to the data of GRS 1915+105 to understand whether it behaves as chaos or random. In the next section, we discuss this.

## 3. RESULTS

We take the RXTE data of OIDs corresponding to each of the temporal classes of GRS 1915+105. It is found that different OIDs for a particular class give same results upto an error bar. Therefore, we choose one OID for each temporal class to present our results, given in Table 1. For each class we extract a few continuous data streams  $\sim 3000$  sec long. The time resolution of light-curves is chosen as 0.1 sec, which gives  $\sim 30000$  data points for each of them with  $\sim 1000$  counts per bin. Light-curves for a finer time resolution are Poisson noise dominated, while with a larger binning give a very little number of data points for the present purpose. In our cases, the auto-correlation function neither goes to zero nor attains a minimum, therefore that  $\tau$  is chosen in our calculations above which the  $D_2 - M$  curves saturate. Here this saturated  $\tau$  is typically  $\sim 20 - 50$ , and we choose it as  $\tau = 50$  for all the cases.

In Fig. 1, we show results for seven temporal classes of GRS 1915+105 data following the method outlined in §2. According to the description of chaos, random, and degrees of freedom in Introduction, the solid diagonal line in each of the boxes in the figure indicates the *ideal random curve*,  $D_2 = M$  line, when there is no constraint into the system. Figure 1 shows the results of  $\beta$ ,  $\kappa$ ,  $\lambda$  and  $\mu$  cases those indicate a clear deviation of this ideal random curve which depict a signature of chaos of dimension  $\sim 3.3 - 4.5$ . In contrary, the curve of  $\chi$  case perfectly overlaps with  $D_2 = M$  line which indicates an ideal random signature. Also the temporal classes  $\gamma$  and

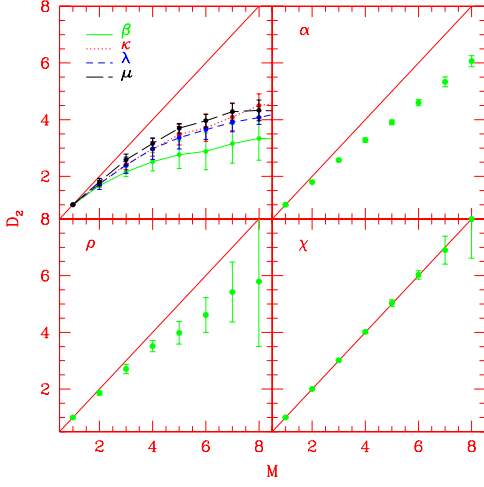


**FIGURE 1.** Results for GRS 1915+105 data in seven temporal classes. The curves for  $\kappa$ ,  $\mu$ ,  $\beta$  and  $\lambda$  classes indicate chaotic signature, while that for  $\chi$  shows random or stochastic nature of the system. The cases for  $\alpha$  and  $\rho$  indicate *some deviation* from random signature.

$\phi$  show a similar random signature. The cases of  $\alpha$  and  $\rho$  show a deviation of the ideal random, but that is not as much as of chaos cases. Therefore we call this kind of situations as semi-random (or semi-stochastic). Similar semi-random behaviors come out from the analysis of  $\theta$ ,  $\nu$  and  $\delta$  temporal classes.

At this point, we could divide the results as well as GRS 1915+105 system into three different classes or stages: low-dimensional chaos (deterministic), random or stochastic (indeterministic) and semi-random, as far as the non-linear dynamical analysis is concern. However, we like to perform a *test* before making any strong statement. We know that the Lorenz system is a model of low dimensional chaos where the chaotic dimension,  $D_2 = 2.04$ . That means for the data of Lorenz system,  $D_2 - M$  curve starts to saturate when  $M = 2$  with the saturation  $D_2$  is 2.04. On the other hand the  $D_2 - M$  curve for the Poisson noise appears as a straight line of unit gradient passing through the origin (i.e.  $D_2 = M$ ). Let us take the Lorenz data set and introduce Poisson noise into it in such a manner that the average count and rms variation become same as that of  $\beta$  case. Then using this modified *noise induced Lorenz data*, if we perform  $D_2 - M$  analysis again, now the surprising fact comes out that  $D_2$  no longer saturates to 2.04, instead becomes increased to  $\sim 4$ . If a higher order rescaling (as mentioned above) to Lorenz data is performed, such that the average count and rms variation are same as that of  $\gamma$  case, the  $D_2$  becomes more and more increased, approached toward the  $D_2 = M$  line though not exactly overlapped on it. All these scenarios have been pictorially represented in

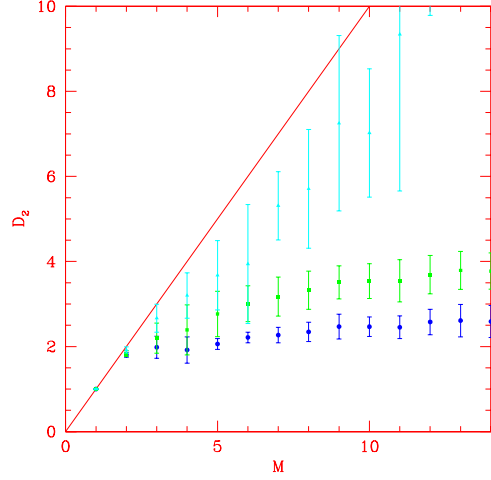


**FIGURE 2.** The effect of Poisson noise to the Lorenz data. The curve with circles indicates the result for actual Lorenz data. The curves with squares and triangles come out when the Lorenz data is rescaled by Poisson noise to  $\beta$  and  $\gamma$  like classes (with the same average count and rms variation).

Fig. 2. From these discussions, it is very clear that presence of any kinds of noise converts any low dimensional chaotic system to that of high dimensional and/or random or semi-random. It does not matter whether the system has any chaotic signature or not, noise always suppress it and the system practically appears as higher dimensional or random. Therefore the computed chaotic dimension  $\sim 4$  (comes out from Fig. 1) is an over estimation. If the noise would have been possible to remove from the system, those could appear as a low dimensional chaos like Lorenz system. Similarly, the random and semi-random appearance of, say,  $\chi$  and  $\alpha$  classes respectively, are only due to the dominance of noise into the system. If the system would have been noise free (or less noisy) those classes could also be appeared as chaos or/and low dimensional chaos. This dominance of noise into the system in the random cases will be more clear if we look on to the Table 1, which clearly shows the Poisson noise to rms ratio is higher for the random cases compared to that for the cases of chaos. The table also lists the various OIDs corresponding to the temporal classes, the average count, rms variation, Poisson noise and finally what the analysis tells about it, whether the system is chaos: C, random/stochastic: S or semi-random/stochastic: SS.

## 4. CONCLUSIONS

We analyze the non-linear behavior of the micro quasar GRS 1915+105 in terms of the signature of chaos and random. It immediately comes out that at least four out of

**TABLE 1.** Columns:- 1. RXTE OID, 2. Temporal class of the system according to [1], 3. Average count in the light-curve,  $\langle S \rangle$ , 4. Root mean square variation in the light-curve,  $rms$ , 5. Expected Poisson noise variation,  $\langle PN \rangle \equiv \sqrt{\langle S \rangle}$ , 6. Ratio of the expected Poisson noise to root mean square variation, 7. Stage of the system as understood from  $D_2 - M$  curves (C: chaotic; SS: semi-stochastic; S: stochastic)

OID	Class	$\langle S \rangle$	$rms$	$\langle PN \rangle$	$\langle PN \rangle / rms$	Stage
10408-01-10-00	$\beta$	1917	1016	43.8	0.04	C
20402-01-37-01	$\lambda$	1493	1015	38.6	0.04	C
20402-01-33-00	$\kappa$	1311	800	36.2	0.04	C
10408-01-08-00	$\mu$	3026	999	55	0.06	C
20402-01-45-02	$\theta$	1740	678	41.7	0.06	SS
10408-01-40-00	$\nu$	1360	462	36.9	0.08	SS
20402-01-03-00	$\rho$	1258	440	35.5	0.08	SS
20187-02-01-00	$\alpha$	582	244	24.1	0.10	SS
10408-01-17-00	$\delta$	1397	377	37.4	0.10	SS
20402-01-56-00	$\gamma$	1848	185	43.0	0.23	S
10408-01-22-00	$\chi$	981	118	31.3	0.27	S
10408-01-12-00	$\phi$	1073	118	32.7	0.28	S

its twelve temporal classes are chaotic in nature. Therefore, there is no doubt that GRS 1915+105 behaves as chaos at least in some stages. The three out of those remaining eight classes depict as random while five others show a deviation from random, called as semi-random. By a simple test, i.e. introducing noise into the low dimensional chaotic system, and from the ratio of Poisson noise to rms variation in the data of various classes, it comes out that the random and semi-random cases are noise dominated. Therefore, we can hypothesize that GRS 1915+105 is chaotic in nature. This chaotic signature is suppressed only in some of its stages due to the noise dominance and it appears like random or semi-random, but actually it is not that.

In early, the results of Cyg X-1 data seemed to be random or very high dimension chaos [2]. On the other hand the temporal behavior of Cyg X-1 is very similar to that of the  $\chi$  class of GRS 1915+105, which is noise dominated depicted as random according to our analysis. Therefore, we understand that due to the dominance of noise into the system, Cyg X-1 could not show its chaotic nature, what it could be actually. In an alternative way, we can say that there may be a stochastic component to the variability which dominates for certain temporal states.

Finally, we can conclude that any black hole system may be chaotic in nature. Depending on the order of noise present into the system, it appears either as actual chaos or random. Any random or semi-random nature may not be its fundamental signature. If the noise would have been possible to remove from the system, always it could show an actual chaotic signature. Overall, the identification of chaotic nature of black hole systems has

opened a new window to understand their temporal behavior deeply. In order to have a more concrete knowledge and to upgrade the confidence level, the next step should be to study the corresponding Lyapunov exponent (which is another basic measure of a non-linear system to distinguish the chaos from random) and the associated Kolmogorov entropy.

## ACKNOWLEDGMENTS

Author would like to thank R. Misra, K. P. Harikrishnan, G. Ambika and A. K. Kembhavi for useful discussions and for collaboration on a project of which the work reported here is a part. Thanks are also given to J. Poutanen for useful discussions. The partial support by Academy of Finland grant 80750 to this work is acknowledged.

## REFERENCES

- Belloni, T., Klein-Wolt, M., Méndez, M., van der Klis, M., and van Paradijs, J., *A&A*, **355**, 271–290 (2000).
- Unno, W., Yoneyama, T., Urata, K., Masaki, I., Kondo, M. and Inoue, H., *PASJ*, **42**, 269–278 (1990).
- Timmer, J., Schwarz, U., Voss, H., Wardinski, I., Belloni, T., Hasinger, G., van der Klis, M. and Kurths, J., *PRE*, **61**, 1342–1352 (2000).
- Thiel, M., Romano, M., Schwarz, U., Kurths, J., Hasinger, G. and Belloni, T., *ApSSS*, **276**, 187–188 (2001).
- Winters, W., Balbus, S. and Hawley, J., *MNRAS*, **340**, 519–524 (2003).
- Misra, R., Harikrishnan, K., Mukhopadhyay, B., Ambika, G. and Kembhavi, A., *ApJ*, **to appear** (2004).